Int. J. Appl. Math. Comput. Sci., 2017, Vol. 27, No. 3, 591–603
DOI: 10.1515/amcs-2017-0042

A COLUMN GENERATION TECHNIQUE FOR ROUTING AND SPECTRUM ALLOCATION IN CLOUD–READY SURVIVABLE ELASTIC OPTICAL NETWORKS

RÓŻA GOŚCIEŃ [a,*], KRZYSZTOF WALKOWIAK [a]

[a]Department of Systems and Computer Networks, Faculty of Electronics
Wrocław University of Science and Technology, Wybrzeże Wyspiańskiego 27, 50-370 Wrocław, Poland
e-mail: roza.goscien@pwr.edu.pl

Driven by increasing user requirements and expectations, the fast development of telecommunications networks brings new challenging optimization problems. One of them is routing and spectrum allocation (RSA) of three types of network flows (unicast, anycast, multicast) in elastic optical networks (EONs) implementing dedicated path protection (DPP). In the paper, we model this problem as integer linear programming (ILP) and we introduce two new optimization approaches—a dedicated heuristic algorithm and a column generation (CG)-based method. Then, relying on extensive simulations, we compare algorithm performance with reference methods and evaluate CG efficiency in detail. The results show that the proposed CG method significantly outperforms reference algorithms and achieves results very close to optimal ones (the average distance to optimal results was at most 2.1%).

Keywords: elastic optical network, anycast traffic, multicast traffic, network survivability, column generation technique.

1. Introdution

Year by year we observe that the profile and expectations of telecommunications network users are changing. We also notice that the number of users increases very fast. Alongside, the number of devices connected to networks also rises, since users are especially interested in mobile communication that can be reached by means of numerous devices—laptops, smartphones, tablets, etc. Concurrently, users are more and more interested in new, bandwidth-intensive services related to data centers (DCs) and content distribution (especially video distribution). The most representative examples of these services are cloud computing, computing grids, Internet video, software distribution, etc. (cf. Zhao *et al.*, 2014; Kobusińska *et al.*, 2016). As a consequence of these trends, the global network traffic increases very fast. The Cisco company forecasts that the global IP traffic will nearly treble over the next five years (Cisco, 2016). Additionally, since the networks are increasingly popular, it is expected that they should work continuously without any outages. The above-mentioned trends reveal requirements that the network operators have to take into account in order to adapt their networks to incoming expectations. Since the currently applied mechanisms and technologies are not efficient enough for future networks, it is required to implement some improvements in both network infrastructures and traffic engineering tools.

Considering network architectures, the idea of elastic optical networks (EONs) is expected to be a beneficial answer for future optical networks (Jinno *et al.*, 2010). The EON combines advantages of advanced transmission techniques and flexible frequency grids. By these means, it brings better spectrum utilization compared with the technology deployed nowadays (wavelength division multiplexing, WDM) (Jinno *et al.*, 2010). In EONs, the available spectrum width is divided into narrow, same-size (6.25 or 12.5 GHz (ITU-T, 2012)) segments, called *slices*. A number of adjacent slices creates a channel that can be used to transmit data. Next, regarding traffic engineering tools, it can be beneficial to apply different transmission types conforming to the characteristics of the realized services (Kmiecik *et al.*, 2014; Walkowiak, 2010). The simplest and the most popular transmission is *unicasting* defined as a point-to-point data exchange. It can be adapted to realize almost all services; however, it is inefficient for DC- and content-related services. Here,

*Corresponding author

much more beneficial is the application of anycast and multicast traffic. In anycasting, we are given a set of DCs, i.e., nodes that are related with servers that can provide some content/service. Since all DCs provide exactly the same content/service, a network node interested in this facility (i.e., anycast client) can establish a connection with any of the DCs. Thus, it is known as one-to-one of many transmission (Walkowiak, 2010). Concurrently, in multicasting, one node that can provide some content (root node) sends it to a group of interested receivers. Hence, it is known as one-to-many transmission (Kmiecik *et al*., 2014). Finally, since networks rely on elements that are likely to fail, it is impossible to avoid any network failures. Thus, survivability mechanisms are required to alleviate failure repercussions and restore network connectivity. One of the most popular and efficient survivability mechanisms is dedicated path protection (DPP), which assigns each traffic demand additional resources (besides normal resources) that allow realizing it in case of a failure (Goścień *et al*., 2014).

The EON technology also brings a new challenging optimization problem called routing and spectrum allocation (RSA) (Christodoulopoulos *et al*., 2011). It concerns assigning a light-structure to each traffic demand. The light-structure is a connection of a routing structure, which allows routing a demand over a network, and a frequency channel. For a unicast demand the routing structure is defined as a routing path that originates in the demand source node and terminates in its destination node. For an anycast demand, first a DC has to be selected (one of all available ones). Then, two routing paths are necessary: from the client node to the selected DC (upstream) and from the selected DC to the client node (downstream) (Goścień *et al*., 2014). Eventually, a routing structure for a multicast demand is defined as a routing tree that originates in the demand root node and contains all its receivers (Walkowiak *et al*., 2015). Additionally, when the DPP scheme is implemented in the network to protect it against a single link failure, the aim of RSA is to assign a pair of link-disjoint light-structures to each demand (Goścień *et al*., 2014). RSA has proved to be NP-complete in general (Christodoulopoulos *et al*., 2011); therefore, efficient solution methods are required. Exact methods (e.g., based on mathematical models such as integer linear programming (ILP)) do not scale up well and are able to solve only unrealistically small problem instances (Walkowiak *et al*., 2015). Hence, some large-scale optimization approaches are necessary. Here, the column generation (CG) technique seems to be a promising approach, since it has been successfully applied to different optimization problems (Klinkowski *et al*., 2016; Ruiz *et al*., 2013; Żotkiewicz *et al*., 2015).

In this paper, we study a novel optimization problem entailed by the development of telecommunication networks. The problem is RSA with three types of network flows (unicast, anycast, multicast) in an EON implementing the DPP scheme to protect flows against a single link failure. We model the problem as an ILP and propose two solution methods: a dedicated heuristic algorithm and a column generation-based approach. Then, we perform numerical experiments in order to compare the methods performance with reference algorithms and evaluate in detail column generation efficiency.

The main novelty and contribution is three-fold. First, we formulate and model a new optimization problem of joint allocation of three types of demands (unicast, anycast, multicast) in an EON under the DPP scheme. We focus on two-directional anycasting (traffic from the DC to the client and from the client to the DC). Second, for the problem we propose solution methods including an efficient CG-based approach. Third, we perform simulations focused on the comparison of the algorithms performance with respect to the reference methods, as well as detailed analysis of CG efficiency.

The paper is organized as follows. Section 2 presents a review of the related works. Section 3 defines the optimization problem by means of a verbal description and a mathematical model. Then, Section 4 discusses solution algorithms including a column generation-based method. Section 5 presents a results of numerical experiments while the Section 6 concludes the paper.

2. Related works

The EON technology and the RSA problem were widely studied in the literature; however, the majority of related papers considers only unicast flows. The anycast (Zhang and Zhu, 2014; Goścień *et al*., 2014; Lu *et al*., 2015) and multicast (Ruiz and Velasco, 2015; Liu *et al*., 2013; Yang *et al*., 2015) traffic in EONs was also studied, but not so precisely. Also, joint optimization of different types of flows in EONs was studied for the following combinations: unicast together with anycast (Klinkowski and Walkowiak, 2013; Goścień *et al*., 2014), unicast with multicast (Walkowiak *et al*., 2015), anycast with multicast (Klinkowski and Walkowiak, 2015) and three types of flows simultaneously (Aibin *et al*., 2016). To the best of the authors' knowledge, Aibin *et al*. (2016) are the only authors who cover joint optimization of the three types of flows in EONs.

Also survivable EONs were studied in the literature (Shen *et al*., 2016). The research related to the protection in EONs applies, among others, path-based methods (Goścień *et al*., 2014; Chen *et al*., 2015; Wang *et al*., 2015) with respect to two spectrum sharing policies: dedicated protection (Goścień *et al*., 2014; Chen *et al*., 2015) and shared protection (Wang *et al*., 2015). Also regarding survivable EONs a majority of papers focus only on unicast flows. Survivable anycasting was studied, for

instance, by Walkowiak *et al*. (2014) and Goścień *et al*. (2014), while survivable multicasting was covered only in two papers (Kmiecik *et al*., 2014; Cai *et al*., 2015). Joint optimization of at least two types of flows in survivable EONs was studied only for anycast and unicast flows, for instance, by Goścień *et al*. (2014). To the best of the authors' knowledge, there is no paper that covers optimization of multicast together with another traffic type in survivable EONs, or a paper that covers survivable routing of three types of flows.

Eventually, many optimization methods were proposed for problems in communication networks, including methods based on optimization theory (Song *et al*., 2014). Concerning EON related problems, also CG was applied. Klinkowski *et al*. (2016), Ruiz *et al*. (2013) or Velasco *et al*. (2014) focus on efficient methods to solve the problem of allocating unicast demands in an unprotected EON. It is worth mentioning that Ruiz *et al*. (2013) and Velasco *et al*. (2014) apply the CG technique directly to solve RSA while Klinkowski *et al*. (2016) propose a branch-and-price approach that incorporates, among others, CG. Next, Klinkowski *et al*. (2013) focus on optimization of anycast traffic in an unprotected EON wherein they model an anycast demand as a one-directional transmission from a DC to the client node. Recall that in this paper we focus on two-directional anycast transmission. The optimization of more than one traffic type in EONs using CG was considered only by Klinkowski and Walkowiak (2015) for the combination of anycast (modeled as one-directional transmission) and multicast flows in an unprotected EON. CG was applied for a survivable EON only by Żotkiewicz *et al*. (2015); however, the authors focused on restoration of unicast flows after a failure.

Summarizing, to the best of the authors' knowledge, only Aibin *et al*. (2016) focused on joint optimization of three types of flows in EONs, and there is no paper that covers the routing of three types of flows in survivable EONs. Moreover, research related to EONs lacks application of the CG technique to optimization of anycast (especially in two-directional mode) and multicast flows, as well as joint optimization of different traffic types and survivability provisioning. The proposed paper fills the literature gaps.

3. Problem formulation

The problem studied is routing and spectrum allocation (RSA) of three types of flows (unicast, anycast, multicast (UAM)) in an elastic optical network that implements a dedicated path protection (DPP) scheme. The problem acronym name is RSA-UAM-DPP. The problems aims to assign each demand resources that are necessary to realize it—two disjoint light-structures. In the paper, protection against a single link failure is considered; thus two light-structures selected for a demand have to be link-disjoint. What is more, it is assumed that the same channel approach is applied: thus the channels of two selected light-structures have to be located around the same central frequency (Goścień *et al*., 2014).

The problem is considered with respect to two different optimization criteria related to spectrum usage. The first one is the average spectrum usage (Goścień *et al*., 2014) (denoted as AvgSpec) defined as an average index of the highest allocated slice over all links. The second one is the maximum spectrum usage (Goścień *et al*., 2014) (denoted as MaxSpec) defined as the number of slices required to realize all demands (i.e., the index of the highest allocated slice in the network). Note that the value of MaxSpec is determined by the most crowded (in terms of the highest allocated slices) link that is mostly related to a DC node. Hence, MaxSpec does not focus on spectrum usage on less crowded links. On the contrary, AvgSpec takes into account spectrum utilization on all links and achieves averaged utilization. However, it does not take into account variation utilization over different links and utilization on the most crowded link. Thus, the defined criteria are complementary.

The elastic optical network is modelled as a directed graph $G = (V, E)$, where V is a set of network nodes and E is a set of network directed fiber links. On each network link, the available spectrum resources are divided into frequency slices $s \in S$. Based on the available slices, a set of frequency channels $c \in C$ is obtained. Each channel is described by a first slice index, the number of involved slices and a central frequency. The set of channels C contains all channels that can be created with respect to the number of available slices. To serve anycast requests, R network nodes host a DC. It is assumed that the content of all DCs is the same and there is no limit on the number of serving clients by a single DC. Thus, an anycast client can reach the content from any of the available DCs.

A set of static traffic demands $d \in D$ is given. The set contains unicast, anycast and multicast demands. Each unicast demand $d \in D_{uni}$ is represented by a source node, destination node and volume (in Gbps). Next, each multicast demand $d \in D_{multi}$ is represented by a root node, the set of receivers and its volume (in Gbps). Eventually, each anycast request, represented by a client node, upstream and downstream volumes, is realized by two associated demands—downstream $d \in D_{dn}$ (from the selected DC to the client node) and upstream $d \in D_{up}$ (from the client node to the selected DC). Let us assume that d is an anycast demand (downstream or upstream) and $\tau(d)$ is its associated demand (upstream of downstream). Note that two associated demands d and $\tau(d)$ denote one anycast client that represents aggregated anycast requests issued at a particular node of the backbone network. The upstream demand is utilized to send data to the

DC while the downstream demand carries data provided by the DC to the client. Therefore, traffic on both the associated demands is somehow connected. Based on this observation, it is assumed that both associated demands (d and $\tau(d)$) have to be related to the same DC.

In the modelling, a candidate pairs of routing structures approach is applied, which is an extension of the link-path flow notation (Walkowiak *et al.*, 2015). In particular, a routing structure is a set of network links that allow realizing a demand. For unicast and anycast (after DC selection) demands, a structure corresponds to a routing path which connects communicating nodes. In the case of a multicast demand, a structure is interpreted as a routing tree which originates in the root node and contains all receivers. Since DPP protects the network against a single link failure, each traffic demand has to be realized by two link-disjoint routing structures. Let $p = (b_1, b_2)$ be a pair of routing structures wherein b_1 is a primary one (used in a normal network state) and b_2 is its backup link-disjoint structure (used in the case of a primary structure link failure). In the preprocessing stage, for each demand $d \in D$, a set of its candidate pairs of routing structures $p = (b_1, b_2) \in P_d$ is calculated. In particular, a set of *k* different pairs of routing paths is determined for each pair of network nodes. Therefore, for each unicast demand, *k* different pairs of routing paths are available. Since the anycast demand can be served by any of the available DCs, for each anycast demand *kR* different pairs of routing paths are given. Similarly, for each multicast demand $d \in D_{multi}$, a set of *t* candidate pairs of routing trees is determined. Note that parameters *k* and *t* control the number of candidate pairs of routing structures for demands and, as a consequence, the size of the problem solution space. The candidate pairs of routing structures are generated by the method based on the well-known Dijkstra and Yen k-SP algorithms wherein the applied metrics are related to the link length (in kilometres).

To calculate the number of slices required to realize a demand on a candidate routing structure, the model presented by Politi *et al.* (2012) is used. It describes the required number of slices as a function of the demand volume (bit-rate in Gbps), the structure length (in kilometres) and the modulation applied. Note that the length of a routing tree is the distance between the root node and the most distant receiver (Walkowiak *et al.*, 2015). Six modulation formats are considered: BPSK, QPSK, *x*-QAM, where $x \in \{8, 16, 32, 64\}$. To select a modulation for a demand and its routing structure, the distance-adaptive transmission (DAT) rule is used (Walkowiak, 2016). It applies the most spectrally efficient format which, at the same time, minimizes the number of required regenerators.

Next, let a light-structure $l = (b, c)$ be a pair of a routing structure *b* (primary or backup) and a frequency channel *c* allocated on the structure links. Moreover, let $q = (l_1, l_2)$ be a pair of light-structures that are based on a pair of link-disjoint routing structures $p = (b_1, b_2)$. Hence, a pair of light-structures allows demand allocation in an EON under a DPP. In the paper, for each demand $d \in D$, a set of candidate pairs of light-structures $q = (l_1, l_2) \in Q_d$ is given. It is calculated with respect to the given set of candidate pairs of routing structures ($p = (b_1, b_2) \in P_d$) and a given set of channels ($c \in C$). Note that for a particular demand *d* and its candidate routing structure *p* the number of required slices is calculated according to the DAT rule and only channels of that size are considered. Since the same channel approach is applied, both the channels from a pair of light-structures (related to a primary and backup light-structure) have to be located around the same central frequency.

The ILP model of RSA-UAM-DPP for AvgSpec (RSA-UAM-DPP-AvgSpec) is represented by the formulas (1), (3)–(6), while the model of RSA-UAM-DPP for MaxSpec (RSA-UAM-DPP-MaxSpec) is described by (2), (3)–(5), (7).

Sets and indices:

$e \in E$	network links
$s \in S$	frequency slices
$d \in D$	traffic demands
$d \in D_{dn}$	anycast downstream demands
$d \in D_{up}$	anycast upstream demands
$d \in D_{uni}$	unicast demands
$d \in D_{multi}$	multicast demands
$c \in C$	candidate frequency channels
$p = (b_1, b_2) \in P_d$	pairs of routing structures for demand *d*
$l = (b, c)$	light-structure
$q = (l_1, l_2) \in Q_d$	candidate pairs of light-structures for demand *d*. If $d \in D_{uni}$, they connect its end nodes. If $d \in D_{up}$, they connect the client node and a DC. If $d \in D_{dn}$, they connect a DC and the client node. If $d \in D_{multi}$, they connect its root node and receivers.

Constants:

R	number of available DCSs
α_{le}	= 1 if light-structure *l* uses link *e*; 0 otherwise
β_{ls}	= 1 if light-structure *l* uses slice *s*; 0 otherwise
$\tau(d)$	index of the demand associated with anycast demand *d*
$o(l)/t(l)$	source/destination node of light-path *l*

Variables:

y_{dq}	= 1 if demand *d* is realized using pair *q*; 0 otherwise (binary)
y_e	index of the highest slice used on link *e* (integer)
x_{es}	= 1 if slice *s* is used on link *e*; 0 otherwise (binary)
x_s	= 1 if slice *s* is used on any network link; 0 otherwise (binary)

Objective:

$$\min z_{avg} = \frac{1}{|E|}\sum_{e} y_e. \tag{1}$$

$$\min z_{max} = \sum_{s} x_s. \tag{2}$$

Subject to:

$$\sum_{q\in Q_d} y_{dq} = 1, d \in D, \tag{3}$$

$$\sum_{q=(l_1,l_2)\in Q_d} y_{dq} o(l_1) = \sum_{q=(l_1,l_2)\in Q_{\tau(d)}} y_{\tau(d)q} t(l_1), \quad d \in D_{dn}, \tag{4}$$

$$\sum_{d\in D}\sum_{q=(l_1,l_2)\in Q_d} y_{dq}(\alpha_{l_1 e}\beta_{l_1 s} + \alpha_{l_2 e}\beta_{l_2 s}) \leq x_{es}, \quad e \in E, \quad s \in S, \tag{5}$$

$$s x_{es} \leq y_e, \qquad s \in S, \qquad e \in E \tag{6}$$

$$x_{es} \leq x_s, \qquad s \in S, \qquad e \in E. \tag{7}$$

Equations (1) and (2) define objective functions, i.e., average and maximum spectrum usage, respectively. Then, the formulas (3)–(7) describe problem constraints. Equation (3) guarantees that for each demand exactly one pair of light-structures is selected, while (4) assures that the same DC is selected for both the associated anycast demands (d and $\tau(d)$). Next, (5) defines variable x_{es}, which says if slice s is allocated on link e. Eventually, (6) defines variable y_e which represents the index of the highest allocated slice on link $e \in E$ while (7) defines variable x_s, which tells if slice s is used on any network link.

4. Algorithms

This section presents two novel approaches to solve RSA-UAM-DPP: a heuristic algorithm of adaptive frequency allocation (AFA) and a column generation-based method.

4.1. Adaptive frequency allocation. The proposed AFA is an extension of the method introduced by Goścień *et al*. (2014) with modifications to serve multicast demands. AFA tries to find a beneficial solution based on a dedicated set of metrics and a continuous analysis of the current resource availability. The AFA solution stores the demand allocation order and information about selected pairs of routing structures for demands, as well as DCs for anycast demands. Based on solution data, demands are allocated one by one (according to the demand allocation order) using selected pairs of structures (and DCs) with respect to the first-fit spectrum assignment policy.

Initially, AFA calculates a basic metric n_d for each demand. For unicast and anycast demands, it is the minimum number of slices required to realize the demand. In particular, for each candidate pair of routing structures, AFA sums the number of slices required to realize the demand on this pair. The final metric value is the minimum obtained sum (over all pairs). For an anycast demand, pairs of structures related to all DCs are considered. For a multicast demand, four metric definitions are considered: (i) volume (in Gbps), (ii) volume multiplied by the number of receivers, (iii) volume multiplied by the number of slices (sum of slices necessary for the primary and backup tree) required to realize the demand on the first available pair of routing trees, (iv) volume multiplied by the number of receivers and multiplied by the number of slices required to realize demand using the first available pair of routing trees. Next, a set of collision metrics is obtained for each: link $col\_e(e) \sum_{d\in D}\sum_{q=(l_1,l_2)\in Q_d}(\alpha_{l_1 e} + \alpha_{l_2 e})n_d$, pair of structures $col\_p(p = (b_1, b_2)) = \sum_{e\in b_1 \bigvee e\in b_2} col\_e(e)$ and demand $col\_d(d) = (1/|P_d|)\sum_{p\in P_d} col\_p(p)$.

Afterwards, AFA allocates demands in three loops. Each loop handles a different demand type according to the following order: multicast, unicast, anycast. Since a basic metric has four definitions for multicast demands, the multicast allocation process is repeated four times (for each metric definition) and the definition that provides the lowest value of the objective is used for further calculations. For each traffic type, the allocation process is as follows. First, demands with the same value of the metric n_d are grouped together into sets $B_m = \{d : n_d = m\}$. Then, sets B_m are considered one by one in a decreasing value of m. For each set B_m, its demands are allocated iteratively. To find a demand $d \in B_m$ that currently provides the lowest value of the objective, AFA uses function *FindD*(B_m). It simulates allocation of all demands in B_m and returns the index of the demand d^* that currently provides the best value of the objective. If more than one demand achieves the smallest value, the demand with the lowest value of metric $col\_d(d)$ is selected. Next, the function *FindP*(d^*) finds a pair of routing structures $p^* \in P_{d^*}$ that currently applied for demand d^* provides the lowest value of the objective. If more than one pair provides this value, the pair with the lowest value of metric $col\_p(p)$ is chosen. Then, the demand d^* is allocated to the pair p^* and removed from the set B_m.

4.2. Column generation technique. The column generation technique is a decomposition method which decomposes (reduces) the initial optimization problem into another problem that is characterized by a smaller

number of variables. In the CG notion, a very important term is a *column*, which refers to the problem variable that can be added/removed from the problem formulation. The aim of the CG method is to find a set of columns (variables) that are expected to provide an optimal or sub-optimal solution wherein the set is only a subset of all feasible columns.

In the proposed CG-based algorithm, the column definition refers to a candidate pair of light-structures for a demand. Since the CG method aims at reducing the number of problem variables (columns), it is necessary to describe the optimization problem with a subset of initial variables. Let Q_d be a set of all feasible candidate pairs of light-structures for demand $d \in D$ (feasible columns). Next, let Q_d^{cur} be a set of currently available candidate pairs of light-structures for demand $d \in D$ (pairs that can be used to realize a demand), and let Q_d^{can} be a set of pairs of light-structures that are feasible but currently are not allowed (not available) for the demand. Note that $Q_d^{cur} \subset Q_d$, $Q_d^{can} \subset Q_d$ and $Q_d^{cur} \cap Q_d^{can} = \emptyset$.

The idea of the CG-based method is presented in Algorithm 1. First, a set of initial columns Q_d^{cur} is obtained for each demand $d \in D$ by AFA (Section 4.1). Then, CG iteratively tries to find and add new columns that are expected to improve a solution. In each iteration, a linear programming (LP) relaxation of RSA-UAM-DPP is solved. It is obtained from the initial problem by transforming binary/integer variables into continuous ones. After that, the related dual variables are extracted for the purpose of a pricing problem that aims to find a column $q^* \in Q_d^{can}, d \in D$, which is characterized by the highest (among all columns in $Q_d^{can}, d \in D$) and positive value of the reduced cost function. If there is such a column, it is added to an appropriate set Q_d^{cur} and removed from the corresponding set Q_d^{can}. Then, CG goes to the next iteration. Otherwise, it solves RSA-UAM-DPP for current sets $Q_d^{cur}, d \in D$, and returns the obtained solution as a final one.

4.2.1. Minimization of the average spectrum usage. RSA-UAM-DPP-AvgSpec is denoted by the formulas (8)–(12). Below, for each constraint, a related dual variable is denoted. Note that the problem of LP relaxation is described by the same equations (formulas (8)–(12)); however, the variables y_{dq}, x_{es}, y_e are continuous:

objective

$$\min z_{avg} = \frac{1}{|E|} \sum_e y_e \tag{8}$$

subject to

$$[\lambda_d \in R]: \quad \sum_{q \in Q_d} y_{dq} - 1 = 0, \quad d \in D, \tag{9}$$

Algorithm 1. CG for RSA-UAM-DPP.

1: **for** $d \in D$ **do**
2: Initialize sets Q_d^{cur} using the AFA method
3: **end for**
4: **loop**
5: Solve LP relaxation of RSA-UAM-DPP using sets Q_d^{cur}
6: Extract dual variables and solve the pricing problem
7: **if** exists a pair light-structure q^* to be added to set Q_d^{cur} **then**
8: Add pair q^* to appropriate set Q_d^{can}
9: **else**
10: Break
11: **end if**
12: **end loop**
13: Solve RSA-UAM-DPP for the current sets Q_d^{cur}
14: **return** Solution obtained for RSA-UAM-DPP

$$[\delta_d \in R]: \quad \sum_{q=(l_1,l_2) \in Q_d} y_{dq} o(l_1) - \sum_{q=(l_1,l_2) \in Q_{\tau(d)}} y_{\tau(d)q} t(l_1) = 0, \quad d \in D_{dn}, \tag{10}$$

$$[\gamma_{es} \geq 0]: \quad \sum_{d \in D} \sum_{q=(l_1,l_2) \in Q_d} y_{dq} (\alpha_{l_1 e} \beta_{l_1 s} + \alpha_{l_2 e} \beta_{l_2 s}) - x_{es} \leq 0, \quad e \in E, \quad s \in S, \tag{11}$$

$$[\pi_{es} \geq 0]: \quad s x_{es} - y_e \leq 0, \quad e \in E, \quad s \in S. \tag{12}$$

Next, we have the formula of the Lagrangian function (Lasdon, 1970) obtained for the ILP formulation of RSA-UAM-DPP-AvgSpec and assigned dual variables,

$$\begin{aligned} &L_{AvgSpec}(y_{dq}, y_e, x_{es}, \lambda_d, \delta_d, \gamma_{es}, \pi_{es}) \\ &= -\sum_{d \in D} \lambda_d \\ &+ \sum_{d \in D} \sum_{q=(l_1,l_2) \in Q_d} (\lambda_d + \sum_{e \in E} \sum_{s \in S} \gamma_{es} (\alpha_{l_1 e} \beta_{l_1 s} \\ &+ \alpha_{l_2 e} \beta_{l_2 s})) y_{dq} \\ &+ \sum_{d \in D_{dn}} \sum_{q=(l_1,l_2) \in Q_d} \delta_d o(l_1) y_{dq} \\ &- \sum_{d \in D_{dn}} \sum_{q=(l_1,l_2) \in Q_{\tau(d)}} \delta_d t(l_1) y_{\tau(d)q} \\ &+ \sum_{e \in E} \left(\frac{1}{|E|} - \sum_{s \in S} \pi_{es} \right) y_e + \sum_{e \in E} \sum_{s \in S} (s \pi_{es} - \gamma_{es}) x_{es}. \end{aligned} \tag{13}$$

Note that the first term of the formula corresponds to the objective function while the rest of terms determine the constraints of the dual problem to the LP problem described by the formulas (8)–(12).

The elements presented in the third line of Eqn. (13) determine the reduced cost function used in the pricing problem. In more detail, in the pricing problem for each column $q \in Q_d^{can}, d \in D$, the value of the reduced cost function is calculated according to the formula (14). Note that the formula depends on the demand. The associated anycast demands are considered separately; however, the value of the reduced cost function of an upstream demand is related to the dual variable of its associated demand:

$$\begin{aligned}&\text{reduced\_cost}(q=(l_1,l_2)\in Q_d^{can})\\&=\begin{cases}\lambda_d+\zeta(q) & \text{if } d\in D_{uni}, D_{multi},\\ \lambda_d+\zeta(q)+\delta_d o(l_1) & \text{if } d\in D_{dn},\\ \lambda_d+\zeta(q)-\delta_{\tau(d)}t(l_1) & \text{if } d\in D_{up},\end{cases}\\&\zeta(q=(l_1,l_2))=\sum_{e\in E}\sum_{s\in S}\gamma_{es}(\alpha_{l_1e}\beta_{l_1s}+\alpha_{l_2e}\beta_{l_2s}).\end{aligned} \tag{14}$$

4.2.2. Minimization of the maximum spectrum usage. RSA-UAM-DPP-MaxSpec is defined by the formulas (15)–(19):

objective

$$\min z_{max}=\sum_s x_s \tag{15}$$

subject to

$$[\lambda_d\in R]:\quad \sum_{q\in Q_d} y_{dq}-1=0,\quad d\in D, \tag{16}$$

$$[\delta_d\in R]:\quad \sum_{q=(l_1,l_2)\in Q_d} y_{dq}o(l_1)-\sum_{q=(l_1,l_2)\in Q_{\tau(d)}} y_{\tau(d)q}t(l_1)=0,\quad d\in D_{dn}, \tag{17}$$

$$[\gamma_{es}\geq 0]:\quad \sum_{d\in D}\sum_{q=(l_1,l_2)\in Q_d} y_{dq}(\alpha_{l_1e}\beta_{l_1s}+\alpha_{l_2e}\beta_{l_2s})-x_{es}\leq 0,\quad e\in E,\quad s\in S, \tag{18}$$

$$[\pi_{es}\geq 0]:\quad x_{es}-x_s\leq 0,\quad e\in E,\quad s\in S. \tag{19}$$

For each constraint, a related dual variable is indicated. Note that the problem LP relaxation is described by the same equations (formulas (15)–(19)); however, the variables y_{dq}, x_{es}, x_s are continuous.

Next, we have the formula of the Lagrangian function for the ILP of RSA-UAM-DPP-MaxSpec and assigned dual variables:

$$\begin{aligned}&L_{MaxSpec}(y_{dq},x_s,x_{es},\lambda_d,\delta_d,\gamma_{es},\pi_{es})\\&=-\sum_{d\in D}\lambda_d+\sum_{d\in D}\sum_{q=(l_1,l_2)\in Q_d}(\lambda_d\\&+\sum_{e\in E}\sum_{s\in S}\gamma_{es}(\alpha_{l_1e}\beta_{l_1s}+\alpha_{l_2e}\beta_{l_2s}))y_{dq}\\&+\sum_{d\in D_{dn}}\sum_{q=(l_1,l_2)\in Q_d}\delta_d o(l_1)y_{dq}\\&-\sum_{d\in D_{dn}}\sum_{q=(l_1,l_2)\in Q_{\tau(d)}}\delta_d t(l_1)y_{\tau(d)q}\\&+\sum_{s\in S}(1-\sum_{e\in E}\pi_{es})x_s\\&+\sum_{e\in E}\sum_{s\in S}(\pi_{es}-\gamma_{es})x_{es}.\end{aligned} \tag{20}$$

In much the same may as for the AvgSpec (Eqn. (13)), the first element of the formula corresponds to the objective while the other terms determine the constraints of the dual problem to the LP problem described by the formulas (15)–(19). The formula (20) is very similar to that for AvgSpec (Eqn. (13)). The difference is observed in the last two elements of the sum. Hence, the reduced cost function for MaxSpec is described by exactly the same formula as for AvgSpec (Eqn. (14)).

5. Results

This section presents the results of experiments focused on the comparison of the RSA-UAM-DPP solution methods (including AFA and the CG-based approach), as well as a detailed analysis of CG efficiency.

5.1. Simulation setup. We use three realistic network topologies: DT14 (14 nodes, 46 links) (Walkowiak, 2016), NSF15 (15 nodes, 46 links) (NLANR, 2007) and Euro16 (16 nodes, 48 links) (Hofmann and Beaumont, 2005). It is assumed that some nodes host a DC which can provide anycast requests. Scenarios with $R = 2, 3, 4$ DCs are used. For each value of *R*, we consider two different DC locations (a DC location refers to the indices of nodes in which the DCs are placed). Overall, for each topology, we use six different DC locations wherein the nodes with relatively high nodal degrees are chosen to host DCs.

For each topology and each objective function a group of 120 different traffic scenarios is given. The total traffic volume in each scenario is constant (see

Table 1), however, it is divided into unicast, anycast and multicast demands. To describe the amount of a particular traffic type in each scenario, the notation of the traffic pattern $uu/aa/mm$ is applied. It brings information about the percentage ratio of the traffic type (uu—unicast, aa—anycast, mm—multicast) in the overall traffic volume. The scenarios with $uu, aa, mm = 0\%, 33.(3)\%, 66.(6)\%, 100\%$ are used. Note that $uu + aa + mm = 100\%$, hence 10 different versions of a traffic pattern are considered wherein for each version two different sets of demands are defined. The volume of an anycast request is the sum of its downstream and upstream volumes, while the volume of a multicast request is calculated as its volume multiplied by the number of receivers. The demand volumes are selected randomly from the range 10–400 Gbps. The demand end nodes (i.e., sources and destinations of unicast demands, client nodes of anycast demands, roots and receivers of multicast demands) are also selected randomly. Taking into account six DC locations, 10 versions of traffic pattern and two demand sets for a traffic pattern, the number of scenarios (for each topology and objective) is 120. Each scenario is analysed using the following number of available pairs of routing structures: ($k = 2, t = 10$) and ($k = 3, t = 30$).

Table 1. Total traffic volume [Tbps] in simulations.

objective function	DT14	NSF15	Euro16
AvgSpec	3.0	2.4	3.0
MaxSpec	3.3	3.9	3.3

5.2. Elastic optical network assumptions. The EON uses the PDM-OFDM technology with multiple modulation formats selected adaptively among BPSK, QPSK, and x-QAM, $x \in \{8, 16, 32, 64\}$. Here, the spectral efficiency is equal to $1, 2, \ldots, 6$ b/s/Hz, respectively, for these modulations and polarization division multiplexing (PDM), which allows us to double the spectral efficiency. BV-T can combine a number of contiguous subcarriers modulated with the same format and allocated to serve a given bit-rate. A subcarrier occupies 12.5 GHz (Palkopoulou *et al.*, 2012). The EON operates within a flexible ITU-T grid of 6.25 GHz granularity (ITU-T, 2012). Three types of BV-T are used, each described by a different capacity limit: 40, 100 and 400 Gbps. In all scenarios, the transmission reach is extended by means of regenerators that are used only if necessary and if the transmission reach of the lowest-level modulation, among the available ones, is shorter than the structure length. The regenerators are located in network nodes and they do not perform spectrum/modulation conversion. A 12.5 GHz guard-band is used between neighbouring connections (Palkopoulou *et al.*, 2012).

5.3. Comparison of the algorithms. The first goal of the simulations was to compare the algorithms. In this part of the study, besides the CG and AFA approaches, three reference methods were used. The methods are heuristics that were proposed for the pure RSA and adapted to RSA-UAM-DPP: first fit (FF) (Jinno *et al.*, 2010), most subcarriers first (MSF) (Christodoulopoulos *et al.*, 2011) and longest path first (LPF) (Christodoulopoulos *et al.*, 2011). FF allocates demands one by one (according to the order in which they are saved in input data) to the first available resources. Next, MSF sorts demands in a decreasing order of their spectrum requirements and then allocates them to the resources that currently provide the smallest values of the objective. Finally, LPF works similarly to MSF, however, it sorts demands in decreasing length of their candidate routing structures.

To compare the algorithms, all methods were run for scenarios defined for DT14, NSF15 and Euro16. For all scenarios, also the IBM CPLEX solver (version 12.5) with implemented ILP models was run. For $k = 2$, $t = 10$, its processing time was unlimited. Thus, the obtained results are optimal. Since ILP modelling does not scale up well and the CPLEX processing time increases very fast with increasing problem size, its calculations for $k = 3, t = 30$ were limited to 1 hour (for a single scenario) and the obtained results have no guarantee of optimality.

Figures 1 and 2 present a comparison of the algorithms in terms of the gap to the ILP result, which is defined as the difference between the algorithm result and the ILP result, divided by the ILP result. The comparison is presented for $k = 2, t = 10$. Thus the reference ILP results are optimal. Next, Tables 2 and 3 extend the comparison results and report the obtained value of the objective function, the gap to ILP result and processing time for all the cases studied. The presented values are averaged over 120 scenarios. The results show that the proposed CG approach performs very well and significantly outperforms the reference methods. It produced the lowest values of the objective function (among non-exact methods) that are very close to results yielded by CPLEX. The average CG produced to optimal result ($k = 2, t = 10$) was at most 2.1% for both the objectives. Regarding processing time, the heuristic methods run very fast and solve a problem instance in less than 1 s. However, the quality of their results is not very good. CG needs significantly more time to solve a problem instance; however, its processing time is much shorter than that of CPLEX (especially for $k = 3, t = 30$ when CPLEX was not able to terminate in several hours). What is more, the CG results are of high quality and are very close to the ILP ones.

It is also worth mentioning that a majority of solutions returned by CG are optimal. Figure 3 presents ratios of optimal solutions that CG found (with respect to all results). According to the figure, the CG found

Table 2. Performance of the algorithms for AvgSpec: average objective value, average gap to the ILP result, processing time.

	DT14		NSF15		Euro16	
	$k=2,t=10$	$k=3,t=30$	$k=2,t=10$	$k=3,t=30$	$k=2,t=10$	$k=3,t=30$
Average objective value						
ILP	10.1	9.9	16.6	15.4	15.1	14.3
CG	10.5	10.0	16.8	15.7	15.3	14.5
AFA	12.1	12.5	21.8	21.1	20.4	19.5
MSF	16.1	15.9	22.9	23.8	28.6	30.2
LPF	13.1	13.2	21.3	21.5	22.3	22.9
FF	16.4	16.4	25.9	25.9	28.7	28.7
Average gap to ILP result						
ILP optimality gap	0.0%	5.2%	0.0%	1.8%	0.0%	3.9%
CG	1.4%	1.5%	2.1%	1.9%	1.1%	1.5%
AFA	26.6%	27.9%	31.2%	35.2%	34.7%	36.2%
MSF	61.4%	67.1%	39.5%	54.9%	101.5%	124.0%
LPF	33.4%	40.8%	29.4%	40.8%	60.2%	71.6%
FF	63.7%	69.9%	63.3%	76.1%	106.8%	115.9%
Average processing time [s]						
ILP	2389.2	3600.0*	1880.2	3600.0*	2649.1	3600.0*
CG	897.5	1642.8	1352.9	791.4	1128.1	1227.9
AFA, MSF, LPF, FF	< 0.2					

* processing time limited to 1 hour

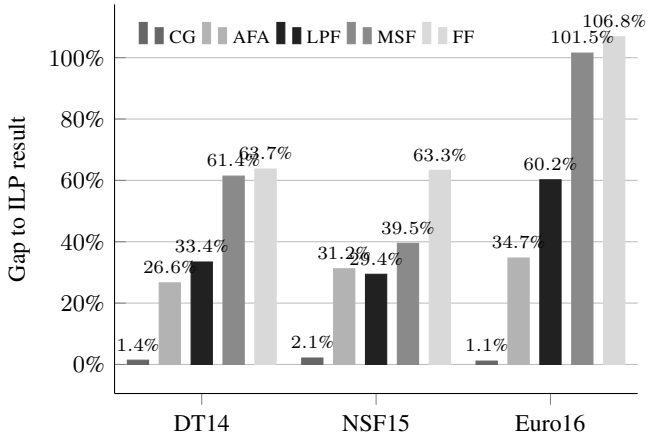

Fig. 1. Gap to the ILP result for $k = 2, t = 10$ and AvgSpec.

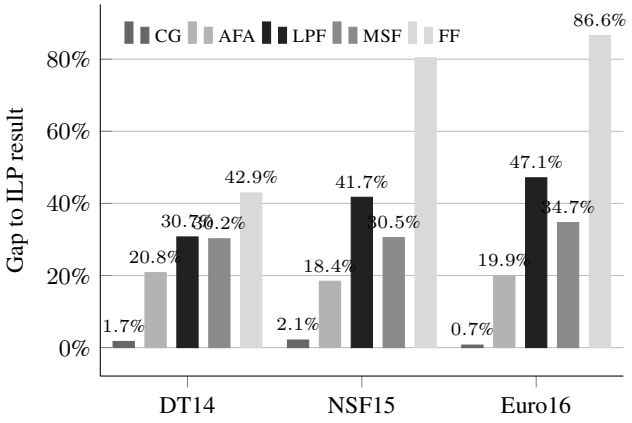

Fig. 2. Gap to the ILP result for $k = 2, t = 10$ and MaxSpec.

up to almost 77% optimal solutions (Euro16, MaxSpec). Note that CG found more optimal solutions for MaxSpec than for AvgSpec. The rest of the methods (AFA, MSF, LPF, FF) performed much worse in this comparison and reached up to 5% of optimal solutions for AvgSpec and up to 15% for MaxSpec.

The above-discussed results can produce a hypothesis that CG is the best method among all non-exact tested approaches. To verify this hypothesis, statistical analysis was performed. Table 4 reports average ranking of the methods after the Friedman test (Derrac *et al.*, 2011). For each configuration, the lowest rank is marked in bold. Next, Table 5 reports pairs of methods for which the differences between their obtained results are not statistically important (based on the Shaffer test with $\alpha = 0.05$ level of significance (Derrac *et al.*, 2011) and ranking after the Friedman test). According to the results, the CG rank is always the smallest and very close to 1 while the differences between CG results and results of any other non-exact method are statistically important. Hence, the statistical analysis proves the hypothesis that the proposed CG is most efficient among all tested methods.

5.4. Efficiency of the column generation process. The second goal of the simulations was to evaluate CG efficiency in detail. Recall that CG aims at reducing the number of variables in the ILP problem formulation by selecting only variables that are expected to provide a good-quality solution. Then, for the reduced set of

Table 3. Performance of the algorithms for MaxSpec: average objective value, average gap to the ILP result, processing time.

	DT14		NSF15		Euro16	
	$k=2,t=10$	$k=3,t=30$	$k=2,t=10$	$k=3,t=30$	$k=2,t=10$	$k=3,t=30$
Average objective value						
ILP	31.2	30.3	53.8	50.9	44.7	40.3
CG	31.4	30.9	55.5	51.4	44.6	40.9
AFA	36.6	36.4	62.4	59.2	51.9	47.3
MSF	38.2	39.8	68.2	65.0	57.3	58.0
LPF	39.0	39.0	73.4	69.0	62.1	61.4
FF	42.4	42.4	93.3	93.3	77.8	77.8
Average gap to ILP result						
ILP optimality gap	0.0%	1.5%	0.0%	5.2%	0.0%	4.0%
CG	1.7%	2.0%	2.1%	1.2%	0.7%	1.4%
AFA	20.8%	22.8%	18.4%	18.4%	19.9%	21.3%
MSF	30.2%	47.5%	30.5%	32.7%	34.7%	52.4%
LPF	30.7%	35.4%	41.7%	42.2%	47.1%	61.7%
FF	42.9%	47.5%	80.4%	94.5%	86.6%	109.3%
Average processing time [s]						
ILP	2389.2	3600.0*	5378.5	3600.0*	3592.0	3600.0*
CG	848.7	1995.5	1158.2	4440.2	1309.0	3289.5
AFA, MSF, LPF, FF	< 0.2					

* processing time limited to 1 hour

Table 4. Performance of the algorithms: average ranking after the Friedman test.

	DT14		NSF15		Euro16	
	$k=2,t=10$	$k=3,t=30$	$k=2,t=10$	$k=3,t=30$	$k=2,t=10$	$k=3,t=30$
AvgSpec						
CG	**1.05**	**1.06**	**1.01**	**1.00**	**1.02**	**1.00**
AFA	2.77	2.77	3.04	2.82	2.60	2.45
MSF	4.13	4.08	3.76	3.72	4.32	4.49
LPF	2.73	2.83	2.89	3.00	2.98	3.05
FF	4.32	4.28	4.48	4.46	4.08	4.01
MaxSpec						
CG	**1.20**	**1.15**	**1.12**	**1.00**	**1.11**	**1.10**
AFA	2.59	2.58	2.43	2.30	2.47	2.20
MSF	3.34	3.55	3.05	3.23	3.10	3.38
LPF	3.60	3.47	3.49	3.60	3.79	3.65
FF	4.27	4.35	4.91	4.86	4.53	4.68

variables, the ILP model implemented in CPLEX is used to find a problem solution. The fewer variables are included in the model, the less complex problem instance is and the fewer computational resources are necessary to solve it by means of ILP. Hence, the CG process can extend the applicability of the ILP formulation as a method to find a problem solution. In this section, we investigate how efficiently CG reduces the size of problem instances.

Table 6 summarizes the CG results according to the efficiency of the reduction in the number of columns. In particular, for each testing scenario, three values are saved: the number of variables in its full ILP formulation (denoted as "initial columns"), the number of variables after the CG process ("end columns") and the column reduction ratio ("column reduction gain") defined as the difference between the number of columns in the full ILP formulation and the number of columns after the CG process, divided by the number of columns in the full model. The three above-mentioned values are averaged over 120 scenarios and presented in Table 6.

The results prove that the CG process can very efficiently decrease the size of the ILP problem formulation by reducing the number of columns up to almost 80% (the highest gain observed for Euro16, MaxSpec, $k = 2, t = 10$). The gains do not vary much for different network topologies. It can be also expected that gains increase with topology size (number of nodes); however, the results for AvgSpec and $k = 2, t = 10$ do not underpin this observation.

Table 5. Pairs of algorithms for which the differences between the obtained results are not statistically important based on the Schaffer test with an $\alpha = 0.05$ level of confidence and ranking after the Friedman test (Table 4).

	AvgSpec			MaxSpec		
	DT14	NSF15	Euro16	DT14	NSF15	Euro16
$k = 2, t = 10$	FF-MSF, LPF-AFA	LPF-AFA	LPF-AFA, FF-MSF	MSF-LPF	—	—
$k = 3, t = 30$	FF-MSF, LPF-AFA	LPF-AFA	—	MSF-LPF	MSF-LPF	MSF-LPF

Table 6. CG performance for small scenarios: efficiency of the reduction of the number of columns.

	DT14		NSF15		Euro16	
	$k = 2, t = 10$	$k = 3, t = 30$	$k = 2, t = 10$	$k = 3, t = 30$	$k = 2, t = 10$	$k = 3, t = 30$
AvgSpec						
initial columns	2314	3803	1538	3178	1809	4008
end columns	603	1379	463	1000	466	1366
columns reduction gain	66.0%	63.5%	67.9%	70.6%	72.5%	66.4%
MaxSpec						
initial column	3880	6326	2599	5342	2677	6245
end columns	800	2022	577	1770	523	1954
columns reduction gain	74.7%	66.4%	75.2%	66.6%	79.0%	70.6%

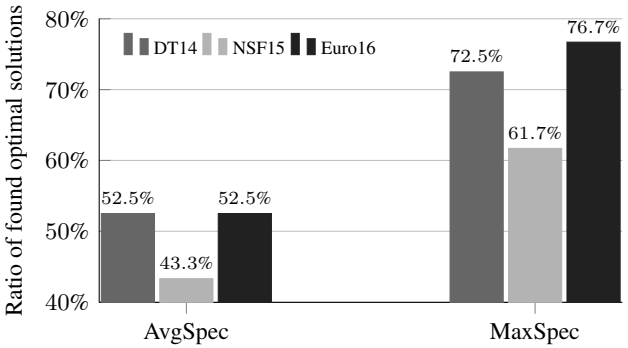

Fig. 3. Ratio of optimal solutions found by the CG algorithm for $k = 2, t = 10$.

6. Conclusions

This paper has focused on the problem of allocating three types of network flows (unicast, anycast, multicast) in an EON that implements the DPP scheme. Since the problem is challenging, we proposed to solve it by means of a dedicated heuristic AFA and an algorithm based on the CG technique. In the paper, we presented the methods in detail, as well as the whole necessary mathematical background. Then, we reported the results of simulations performed to compare the proposed algorithms with the reference methods and to evaluate in detail the CG performance. The results of the investigation show that the proposed CG-based method significantly outperforms the reference approaches and finds solutions very close to optimal ones. For the CG method considered, the average gap to the optimal result was less than 2.1% (for AvgSpec and MaxSpec), while the average distance of the reference methods was at least 28%. Also, the statistical analysis proves good performance of CG. The CG rank after our Friedman test was always smallest and very close to one, while the differences between the CG results and those of any other method were always statistically significant. In future work, we plan to further investigate and improve the performance of the proposed CG method. More specifically, we plan to investigate how the quality of the initial set of columns influences the CG performance. We also plan to design and implement a heuristic method to find a problem solution for a reduced set of columns (instead of the ILP).

Acknowledgment

This work was supported by the Polish National Science Centre (NCN) under the grant DEC-2015/19/N/ST6/01196. This article is based in part upon work from COST Action CA15127 (*Resilient Communication Services Protecting End-User Applications from Disaster-Based Failures—RECODIS*) supported by COST (European Cooperation in Science and Technology).

References

Aibin, M., Goścień, R. and Walkowiak, K. (2016). Multicasting versus anycasting: How to efficiently deliver content in elastic optical networks, *International Conference on Transparent Optical Networks (ICTON), Trento, Italy*, pp. 1–4.

Cai, A., Zukerman, M., Lin, R. and Shen, G. (2015). Survivable multicast and spectrum assignment in light-tree-based elastic optical networks, *Asia Communications and Photonics (ACP), Hong Kong, China*, p. ASu4E.1.

Chen, X., Tornatore, M., Zhu, S., Ji, F., Zhou, W., Chen, C., Hu, D., Jiang, L. and Zhu, Z. (2015). Flexbile availability-aware differentiated protection in software-defined elastic optical networks, *Journal of Lightwave Technology* **33**(18): 3872–3882.

Christodoulopoulos, K., Tomkos, I. and Varvarigos, E. (2011). Elastic bandwidth allocation in flexible OFDM-based optical networks, *IEEE/OSA Journal of Lightwave Technology* **29**(9): 1354–1366.

Cisco (2016). Cisco visual network index: Forecast and methodology, 2015–2020, `https://www.cisco.com/c/en/us/solutions/collateral/service-provider/visual-networking-index-vni/complete-white-paper-c11-481360.html`.

Derrac, J., García, S., Molina, D. and Herrera, F. (2011). A practical tutorial on the use of nonparametric statistical tests as a methodology for comparing evolutionary and swarm intelligence algorithms, *Swarm and Evolutionary Computation* **1**(1): 3–18.

Goścień, R., Walkowiak, K. and Klinkowski, M. (2014). Joint anycast and unicast routing and spectrum allocation with dedicated path protection in elastic optical networks, *Conference on Design of Reliable Communication Networks (DRCN), Gent, Belgium*, pp. 1–8.

Hofmann, M. and Beaumont, L. (2005). *Content Networking: Architecture, Protocols, and Practice,* Morgan Kaufmann, Burlington, MA.

ITU-T (2012). ITU-T recommendation G.694.1. (Ed. 2.0), Spectral grids for WDM applications: DWDM frequency grid, `https://www.itu.int/rec/T-REC-G.694.1/en`.

Jinno, M., Kozicki, B., Takara, H., Watanabe, A., Sone, Y., Tanaka, T. and Hirano, A. (2010). Distance-adaptive spectrum resource allocation in spectrum-sliced elastic optical path network, *IEEE Communications Magazine* **48**(8): 138–145.

Klinkowski, M. and Walkowiak, K. (2013). On the advantages of elastic optical networks for provisioning of cloud computing traffic, *IEEE Network* **27**(6): 44–51.

Klinkowski, M. and Walkowiak, K. (2015). A column generation-based optimization of anycast and multicast traffic in distance-adaptive flexgrid networks, *Asia Communications and Photonics (ACP), Hong Kong, China*, p. AS4H.3.

Klinkowski, M., Walkowiak, K. and Goścień, R. (2013). Optimization algorithms for data center location problem in elastic optical networks, *International Conference on Transparent Optical Networks (ICTON), Cartagena, Spain*, pp. 1–5.

Klinkowski, M., Żotkiewicz, M., Walkowiak, K., Pióro, M., Ruiz, M. and Velasco, L. (2016). Solving large instances of the RSA problem in flexgrid elastic optical networks, *Journal of Optical Communication and Networking* **8**(5): 320–330.

Kmiecik, W., Goścień, R., Walkowiak, K. and Klinkowski, M. (2014). Two-layer optimization of survivable overlay multicasting in elastic optical networks, *Optical Switching and Networking* **14**: 164–178.

Kobusińska, A., Brzeziński, J., Boroń, M., Inatlewski, Ł., Jabczyński, M. and Maciejewski, M. (2016). A branch hash function as a method of message synchronization in anonymous P2P conversations, *International Journal of Applied Mathematics and Computer Science* **26**(2): 479–493, DOI: 10.1515/amcs-2016-0034.

Lasdon, L.S (1970). *Optimization Theory for Large Systems*, Dover Publications, Mineola, NY.

Liu, X., Gong, L. and Zhu, Z. (2013). On the spectrum-efficient overlay multicast in elastic optical networks built with multicast-incapable switches, *IEEE Communications Letters* **7**(9): 1860–1863.

Lu, P., Zhang, L., Liu, Z., Yao, J. and Zhu, Z. (2015). Highly efficient data migration and backup for big data applications in elastic optical inter-data-center networks, *IEEE Network* **29**(5): 36–42.

NLANR (2007). National laboratory for applied network research (NLANR) project, *Technical report*, NSFNET—the National Science Foundation Network, `http://moat.nlanr.net/`.

Palkopoulou, E., Angelou, M., Klonidis, D., Christodoulopoulos, K., Klekamp, A., Buchali, F., Varvarigos, E. and Tomkos, I. (2012). Quantifying spectrum, cost, and energy efficiency in fixed-grid and flex-grid networks, *Journal of Optical Communications and Networking* **4**(11): B42–B51.

Politi, C., Anagnostopoulos, V., Matrakidis, C., Stavdas, A., Lord, A., Lopez, V. and Fernandez-Palacios, J.P. (2012). Dynamic operation of flexi-grid OFDM-based networks, *Optical Fiber Conference (OFC), Los Angeles, CA, USA*, p. OTh3B.2.

Ruiz, M., Pióro, M., Żotkiewicz, M., Klinkowski, M. and Velasco, L. (2013). Column generation algorithm for rsa problems in flexgrid optical networks, *Photonic Network Communications* **26**(2): 53–64.

Ruiz, M. and Velasco, L. (2015). Serving multicast requests on single-layer and multilayer flexgrid networks, *Journal of Optical Communications and Networking* **7**(3): 146–155.

Shen, G., Guo, H. and Bose, S.K. (2016). Survivable elastic optical networks: Survey and perspective (invited), *Photonic Network Communications* **31**(1): 71–87.

Song, F., Huang, D., Zhou, H., Zhang, H. and You, I. (2014). An optimization-based scheme for efficient virtual machine placement, *International Journal of Parallel Programming* **42**(5): 853–872.

Velasco, L., Castro, A., Ruiz, M. and Junyent, G. (2014). Solving routing and spectrum allocation related optimization problems: From off-line to in-operation flexgrid network planning, *Journal of Lightwave Technology* **32**(16): 2780–2795.

Walkowiak, K. (2010). Anycasting in connection-oriented computer networks: Models, algorithms and results, *International Journal of Applied Mathematics and Computer Science* **20**(1): 207–220, DOI: 10.2478/v10006-010-0015-5.

Walkowiak, K. (2016). *Modeling and Optimization of Cloud-Ready and Content-Oriented Networks*, Springer, Berlin.

Walkowiak, K., Goścień, R., Woźniak, M. and Klinkowski, M. (2015). Joint optimization of multicast and unicast flows in elastic optical networks, *IEEE International Conference on Communications (IEEE ICC), London, UK*, pp. 5186–5191.

Walkowiak, K., Kucharzak, M., Kopeć, P. and Kasprzak, A. (2014). ILP model and algorithms for restoration of anycast flows in elastic optical networks, *Reliable Networks Design and Modeling (RNDM), Barcelona, Spain*, pp. 102–106.

Wang, C., Shen, G. and Bose, S.K. (2015). Distance-adaptive dynamic routing and spectrum allocation in elastic optical networks with shared backup path protection, *Journal of Lightwave Technology* **33**(14): 2955–2964.

Yang, L., Gong, L., Zhou, F., Cousin, B., Molnar, M. and Zhu, Z. (2015). Leveraging light forest with rateless network coding to design efficient all-optical multicast schemes for elastic optical networks, *Journal of Lightwave Technology* **33**(18): 3945–3955.

Zhang, L. and Zhu, Z. (2014). Dynamic anycast in inter-datacenter networks over elastic optical infrastructure, *International Conference on Computing, Networking and Communications (ICNC), Honolulu, HI, USA*, pp. 491–495.

Zhao, J., Mhedheb, Y., Tao, J., Jrad, F., Liu, Q. and Streit, A. (2014). Using a vision cognitive algorithm to schedule virtual machines, *International Journal of Applied Mathematics and Computer Science* **24**(3): 535–550, DOI: 10.2478/amcs-2014-0039.

Żotkiewicz, M., Ruiz, M., Klinkowski, M., Pióro, M. and Velasco, L. (2015). Reoptimization of dynamic flexgrid optical networks after link failure repairs, *Journal of Optical Communications and Networking* **7**(1): 49–61.

Róża Goścień received the PhD degree in computer science from the Wrocław University of Science and Technology, Poland, in 2016. Currently, she is an assistant professor at the same university in the Department of Systems and Computer Networks. Her research interest is mainly focused on modelling and optimization of survivable communication networks. She was awarded the 2014 Fabio Neri Best Paper Award from the *Optical Switching and Networking* journal and the Best Paper Award at the *RNDM 2015* conference.

Krzysztof Walkowiak received the PhD and DSc (habilitation) degrees in computer science from the Wrocław University of Science and Technology, Poland, in 2000 and 2008, respectively. Currently, he is an associate professor at the same university in the Department of Systems and Computer Networks. His research interest is mainly focused on modelling and optimization of communication networks. He received the 2014 Fabio Neri the Best Paper Award from the *Optical Switching and Networking* journal and the Best Paper Awards at the *DRCN 2009* and *RNDM 2015* conferences. He has published more than 240 scientific papers in international conference proceedings and journals.

Received: 7 September 2016
Revised: 31 January 2017
Accepted: 23 March 2017